JOURNAL OF GEOPHYSICAL RESEARCH, VOL. ???, XXXX, DOI:10.1029/,

On the Relationship Between Continuing Current and Positive Leader Growth

Jeff L. Lapierre,[1] Richard G. Sonnenfeld,[1] Harald E. Edens,[1] Mike Stock,[1]

Corresponding author: Jeff Lapierre, Department of Physics, New Mexico Institute of Mining and Technology, Socorro, New Mexico, USA. (jlapierr@nmt.edu)

[1]Department of Physics and Langmuir Laboratory, New Mexico Institute of Mining and Technology, Socorro, New Mexico, USA

Abstract. It has long been speculated that the source of continuing current (CC) for a negative cloud-to-ground flash is provided by the growth of its positive leader into negative charge regions. In this study, data from the Langmuir Electric Field Array (LEFA) and Lightning Mapping Array (LMA) are used to investigate these speculations. LEFA and LMA data provide a way to estimate the occurrence and duration of CC and channel growth throughout a flash, respectively. By connecting LMA VHF sources onto contiguous channels, the growth of the positive leader associated with each return stroke is inferred. A linear correlation between positive-channel growth and CC duration is found, providing evidence that the positive leader grows with a constant velocity, but no obvious correlation of this velocity with CC occurrence is found. Each return stroke is then sorted by its channel growth rate and further identified by its CC type. This analysis also provides no identifiable correlation linking the positive-channel growth rate to CC occurrence or duration. Finally, the positive-channel-growth rate for the whole flash is calculated in 10-ms windows so that any trends occurring before, during, or after the CC can be observed. This analysis too shows no correlation, which implies that positive-channel growth is not the primary mechanism that determines CC occurrence and duration.

1. Introduction

1.1. Continuing Current

Cloud-to-ground (CG) flashes consist of leaders that exit the parent cloud and connect to the ground. For a negative CG (–CG) flash, negative charge is carried to ground by a negative leader. Due to the bi-polar nature of lightning, the opposite end (referred to as the positive leader), typically located within the cloud, will be positively charged. When the negative leader connects to ground, it causes a surge of current called the return stroke, which may be followed by a steady, long-lived current called continuing current (CC). Why some return strokes are followed by CC and some are not is still not properly understood, but is thought to depend on the characteristics of the positive leader [*Krehbiel et al.*, 1979; *Rakov and Uman*, 1990; *Mazur*, 2002; *Saba et al.*, 2006a; *Williams*, 2006]. We combined VHF radio emissions measurements (that located regions of electric breakdown of air) with electric field change measurements (which observed charge motion) to study the relationship between the growth of these positive leaders and CCs.

1.2. Continuing Current and the Positive Leader

Among the first to propose a relationship between CC and the positive leader were *Krehbiel et al.* [1979], who suggested, "Because of the highly interactive nature of the discharge process it is likely that both effects (ie., channel negative resistance and availability of source current) are important factors in making the discharge discrete." This statement is very general, however the phrase 'availability of source current' suggests some kind of leader growth in order to connect to additional sources of charge. *Rakov and Uman* [1990] supported this statement, "Given suitable conditions, the alternative between a continuing current and a discrete stroke will then be a matter of the availability of a charge source capable of providing an appropriate current input to the channel." Similarly, in *Rakov and Uman* [2003] on page 176, they stated, "The return stroke removes charge deposited on the channel by a preceding leader, whereas continuing current is likely to be associated with the tapping of fresh charge regions in the cloud". More recently, *Saba et al.* [2006a] stated, "We can speculate that the higher occurrence of long continuing current is related to the availability of charges in the negative charge layer of the thunderstorm and thus to the horizontal extent of the thundercloud." The phrase 'in the negative charge layer' implies that developing positive leaders are the charge source.

Heckman [1992] suggests a model which can be used to determine whether or not a channel can sustain CC. The two critical characteristics for this model are channel length and current on the channel. In summarizing the model developed in *Heckman* [1992], *Williams* [2006] states, "The extension of the channel into the electric field of space charge aloft provides for a quasi-steady current source" [*Williams*, 2006]. Therefore this model depends directly on the positive leader growth to provide sufficient current for CC to occur.

Mazur [2002] stated a direct link between CC and in-cloud leader activity, "The presence of continuing current, commonly observed either in the E-field change record, or as the continuing luminosity of a visible channel, is an indication of a developing leader in the flash. The duration of continuing current, which delineates the duration of leader development, varies from a few to hundreds of ms." They go on to say, "The current source that maintains the arc is associated with the breakdown process at the leader tip and the self-propagation of the leader channel."

Owing to these speculations, the analysis of the positive leader is paramount in understanding CC; the goal of this study.

1.3. Differing Regimes of Continuing Current

The definition of CC duration has been refined over the past several decades. *Brook et al.* [1962] and *Kitagawa et al.* [1962] defined long CC as a continuous electric field change lasting longer than 40 ms. *Shindo and Uman* [1989] then defined short CC as lasting between 10 and 40 ms. They also discussed what they called 'questionable' CC, which was CC that lasted less than 10 ms. However at the time it was difficult to determine if this questionable CC was actually due to CC, in-cloud events, or the tail of the return stroke electric field change. *Rakov and Uman* [2003] determined that the maximum duration of a return stroke was 3 ms, which *Ballarotti et al.* [2005] used to introduce very short CC. They defined very short CC as lasting between 3-10 ms. In this paper we will be using the definitions of long, short, and very short CC which are summarized in Table 1.

1.4. An Intuitive Model

The positive leader grows by the electric breakdown of air due to the large potential difference between the leader tip and the space charge in the cloud. As newly ionized channel grows in conductivity it increasingly approximates an equipotential. As this occurs charges must be redistributed. While we could not find data for positive channels, it has been found that newly formed negative channels have a line charge density between -0.02 mC m^{-1} [*Warner et al.*, 2003] and -1.8 mC m^{-1} [*Lu et al.*, 2011]. These results lead one to suppose that each time a positive leader extends, a similar amount of charge becomes available. Since it is assumed that the channel is grounded, there is a large electric potential difference initially between the old channel and the new channel, which supplies current to the grounded channel as the electric potential equalizes. This picture suggests that current should be proportional to some power of the growth rate. If this is the case, then there should be some measurable increase in positive leader growth during CC compared to when there is none.

2. Instrumentation and Methods

This study focuses on –CG flashes that occurred around Langmuir Laboratory near Socorro, New Mexico. Data from the Langmuir Electric Field Array (LEFA, 0.3 Hz-50 kHz electric field change)[*Sonnenfeld and Hager*, 2013] and Lightning Mapping Array (LMA, 60-66 MHz VHF band)[*Rison et al.*, 1999] are used to analyze the dependence of CC on positive-channel branching and growth. The LEFA is an array of nine slow field change sensors sampling at 50 kHz. Figure 1 illustrates the locations of each station and Langmuir Laboratory, which is considered the origin for our coordinate system. A total of nine flashes, which occurred during the summers of 2012 and 2013, are analyzed. These include 57 return strokes, 30 of which are followed by CC (10 very short, 6 short, and 14 long, per Table 1).

The LEFA data allow us to determine which return stroke was followed by CC and also the duration of the CC. In Figure 2, LEFA3 data for a bolt-from-the-blue flash occurring on 14 August 2012 is plotted, emphasizing the CC, which is represented by the black line segments. We calculate CC duration by measuring the time interval between the return stroke field change and its intersection with interstroke electric field activity (example shown in the inset of Figure 2). The intersection is decided by the measured electric field being within 0.1% of a linear fit to the interstroke electric field. Table 2 summarizes the

CC durations for the 14 August 2012 flash measured at six different LEFA stations. CC durations are shown in order of the distance between each station and the ground strike location (illustrated in the right plot of Figure 9 by a red diamond). Even though LEFA5 is the closest station to the return stroke, we analyze LEFA3 data because of the electric field enhancement due to local terrain variations. LEFA3's location causes the electric field lines to converge and therefore generally gives it the greatest sensitivity of all the stations. Most of the stations are in agreement, however there are some discrepancies, which mainly have to do with the automated calculation of the duration. For example, for RS4, LEFA8, 10, 6, and 7 all measure the electric field waveforms that drop below the inter-stroke electric field before flattening out. This effect causes the automated estimation of the CC duration to be shorter than one would expect from inspection.

When measuring CC durations, high-speed video observations are preferable to E-field data, however, electric field measurements have been shown to also be very effective at observing CC. [*Ross et al.*, 2008]. *Saba et al.* [2006b] showed that the duration of CC determined from high-speed video (CC_{video}) and from electric field measurements ($CC_{\mathrm{E-field}}$) agree. Figure 3 shows this relationship for 19 return strokes, with which they calculated an R-value of 0.87 between the two techniques. This result indicates that E-field measurements are an adequate proxy for estimating CC durations longer than approximately 100 ms. The data provided by *Saba et al.* [2006b] is lacking for CC durations less than 100 ms.

For electric field measurements performed near a lightning flash, it becomes difficult to distinguish between CC and in-cloud activity [*Ross et al.*, 2008]. This is solved by having multiple electric field measurements. The sign of the electric field change measured will depend on the direction of motion of the in-cloud activity relative to the station. The same is not true for CC. Electric field changes for CC are well approximated as monopoles [*Krehbiel et al.*, 1979]. Therefore, if the sign of the electric field change for multiple stations agree, and it resembles what one would expect for CC, then the electric field change in question is due to CC. For example, compare the locations of LEFA3 and LEFA5 (see Figure 1) to the direction of the positive leader in the flash illustrated in Figure 2. The positive leader moves to the north west directly towards LEFA3. Using only LEFA3 data, one would not be able to distinguish if the electric field changes occurring after the third, forth and fifth return strokes were due to CC or the motion of the positive leader. However, since the positive leader motion is perpendicular to LEFA5 and it measures the same sign of electric field change (see Figure 4), one can be confident that CC is the cause of the electric field change. This analysis has been performed for all flashes in this study to legitimize that the electric field changes are due to CC.

LMA data were obtained from the Langmuir LMA comprising 28 stations situated around Langmuir Laboratory. The high number of instruments, along with the relatively quiet environment, gives us the sensitivity required to detect positive breakdown activity, which is much quieter in RF than that produced by the negative leader [*Thomas et al.*, 2004; *Edens et al.*, 2012]. To determine channel growth, we modify the PulseGraph function described in *Hager et al.* [2007]. This function was designed to join LMA VHF source points provided to arrive at a channel structure for a complete flash which can be used to measure channel length. It can also be used to connect new points to an existing channel as the flash progresses in order to calculate the length increase of the channel during the time interval of interest. An example of this analysis is illustrated in Figure 5. Although only the planar view is shown in Figure 5, the LMA provides three-dimensional locations of VHF source points; the channel lengths reported in this paper use three-dimensional data. The red lines on the LEFA and LMA data (left panels) highlight the time of the fifth return stroke, while the red line segments on the PulseGraph figure indicate the new channel growth during that CC. Figure 6 illustrates a plan view comparison between PulseGraph and LMA VHF sources. In order to limit the number of noise solutions and prevent false channel detection by the PulseGraph function, LMA data are filtered using relatively strict parameters of minimum number of stations and reduced chi squared values (typically around 12 and 2 respectively). Applying the PulseGraph function on the filtered LMA data correctly fits the branch structure found in the LMA data and yields the channel lengths used in this analysis. It should be noted that, while the filtering scheme does change the overall magnitude of the channel growth rates, it does not affect the characteristics described in this analysis.

3. Analysis and Discussion

Channel growth is determined for the nine flashes as described above. For each return stroke the time period of CC activity is determined from the LEFA waveform. The PulseGraph algorithm is used to calculate channel growth during that same time interval. The channel growths for all 57 return strokes are plotted in Figure 7 against CC duration. The left panel depicts the data as a base 10 log-log plot while the right panel is a linear plot of the same data. The primary reason for illustrating the data both ways is to show the highly linear dependence (with the log-log plot) while also clearly displaying the cumulative speed of the positive leader (with the linear plot). Calculating the slope of the log-log plot gives us a power law relation of 0.93 (i.e. growth of the positive leader equals duration of CC to the power of 0.93). In other words, the relationship is almost linear. At first glance the data appear to support the accepted hypothesis that CC is caused by the growth of the positive leader because long CCs correspond to large channel growths. However, since the exponent in the left panel of Figure 7 is roughly one, there is a simpler explanation. If the average positive leader branch growth is constant (given by the slope in the right panel of Figure 7), and continues throughout the flash, this linear correlation would also occur. Observations presented later in this paper (seen in Figures 10, 11, and 12) show that the positive leader grows throughout the flash, whether or not there is CC. Therefore, the apparent correlation between long CC and channel growth appears because channel growth of long CCs was calculated for longer periods of time.

Due to this constant positive leader velocity, if the number of branches can be estimated, then an estimate for the positive leader velocity can be found also. The branch analysis begins after the final stepped leader occurs so as not to count branches arising as part of the negative leader. From this time zero, the flash is considered in 100 ms increments. For each increment a branch is considered active if it contains new VHF sources during this time period. The number of branches per time window is averaged over the whole flash, and these are averaged over all the nine flashes in this study. The results obtained from this analysis show that positive leaders have on average approximately 10 active branches.

The slope found in Figure 7 represents the cumulative speed of all the active branches in the positive leader. By dividing this slope by the estimate of the average number of branches in the positive leader found above, an estimate for the velocity of an individual positive leader branch can be found. Therefore,

$$v_{\rm pos} = \frac{R_{\rm tot}}{N_{\rm b}} = \frac{2.1 \times 10^5 \ {\rm ms}^{-1}}{10} = 2.1 \times 10^4 \ {\rm ms}^{-1}, \qquad (1)$$

where v_{pos} is the velocity of the positive leader, R_{tot} is the growth rate of the positive leader (the slope of the waveform(s) in Figure 7), and N_{b} is the estimated average number of branches of the positive leader. The value of 2×10^4 ms^{-1} calculated agrees with what is found in the literature. *Edens et al.* [2012] observed velocities of $1 - 3 \times 10^4$ ms^{-1} in a triggered flash in New Mexico while *van der Velde and Montanyà* [2013] observed horizontal velocities of $1.6 - 2.6 \times 10^4$ ms^{-1} for natural flashes observed in Spain. However, three-dimensional velocities have been observed as high as 3.3×10^6 ms^{-1} [*Yoshida et al.*, 2010].

The data in Figure 7 do not indicate an increase in growth rate during CC, but there was much scatter in the data. Therefore a different approach is taken to find a relationship between growth rate and CC. We explicitly calculate an average growth rate (R_{RS}) for each of the 30 return strokes using

$$R_{\mathrm{RS}} = \frac{G}{t_{\mathrm{CC}}}, \tag{2}$$

where G is the channel growth during the period of return stroke and CC, and t_{CC} is the return stroke and CC duration. Organizing these results into a histogram gives Figure 8. The colors in Figure 8 represent return strokes with long (red), short (green), very short (yellow), or without CC (blue) (according to the definitions of Table 1). Figure 8 is in support of what Figure 7 implied. For the lowest bin (0-250 km s^{-1}), we note that 17 of 29 (59 %) return strokes are followed by CC. Were the prior assumptions about the relation between channel growth and CC valid (per our discussion in Section 1.2), we would assume that the next bin would have a larger fraction of CC strokes, but in fact only 8 of 19 flashes (42 %) are followed by CC. In the three bins with highest growth rates, we have a paucity of data, but there is no evidence that the highest rates provide a larger fraction of CC flashes. Taken as a whole, Figure 8 does not support the assumption that longer CCs correspond with higher positive channel growth rates.

In order to make the best use of our nine flashes, we applied still another form of data analysis. So far, the growth rates were averaged over the time frame of the return stroke and CC. However it is possible to determine the growth rate at higher time resolution. By dividing LMA data for an entire flash into 10 ms windows, the growth rate can then be calculated during those windows. These results are shown in Figures 10, 11 and 12 with the 10 ms growth plotted above the LEFA and LMA data for each flash. This analysis can identify possible trends in growth rate throughout the flash and help to determine if there is a correlation between positive-channel growth and CC not observable in the averaged growth rates from Figure 8.

Figures 6 and 10 illustrate a –CG flash occurring on 8 July 2013. This flash has seven return strokes according to National Lightning Detection Network (NLDN) data (highlighted by vertical blue lines and sequentially numbered in Figure 10), with the first and third return strokes connecting to ground at different locations. The first two return stroke ground points are indicated in Figure 6 by a magenta triangle. The third and subsequent return strokes go to ground at a different location, represented by red diamond in Figure 6. The stepped leaders are apparent in the LMA plot in Figure 10 by the low altitude VHF sources. The channel growth algorithm detects these two stepped leaders as growth maxima, which stand out in the top panel. Inspection of the LMA data show that after the second stepped leader (approximately 1.08 seconds in Figure 10) the growth rate remains constant throughout the rest of the flash. This constant growth rate persists even though the sixth and seventh return strokes are followed by long CC. The constancy of positive-channel growth rate of the 20:28 flash is typical of seven of the nine flashes in this study.

Only two flashes in this study have growth rates that are not constant during positive-channel growth. The first is shown on the left panel of Figure 9 and Figure 11 which occurred on 8 July 2013. This flash has nine return strokes according to NLDN data (highlighted by vertical blue lines and sequentially numbered in Figure 11). There are three different return stroke locations (shown on the left panel of Figure 9). The first two return strokes ground locations are depicted as magenta triangles and and the remaining return strokes by the red diamond. Just as in the 20:28 flash, after the final stepped leader connects to ground (during the third return stroke at 0.525 s) the growth rate decreases and remains relatively constant. Even though the sixth return stroke initiates long CC, the growth rate does not immediately increase. At approximately 0.9 seconds in the figure, about 0.06 seconds after the initiation of the sixth return stroke, the growth rate begins to increase and peaks at around 1 second. There is another peak occurring at around 1.1 seconds, between the seventh and eighth return stroke. Unlike the previous peak this one occurs even though the seventh return stroke is not followed by CC. Finally, the ninth and final return stroke is followed by short CC, but is not accompanied by any appreciable increase in positive-channel growth rate.

The second flash without a constant growth rate is the bolt-from-the-blue discussed earlier, occurring on 14 August 2012, and illustrated on the right panel of Figure 9 and Figure 12. This flash contains six return strokes according to NLDN data (highlighted by vertical blue lines and sequentially numbered in Figure 11), with the third and fourth being followed by short CC and the fifth by long CC. The data show that the growth rate increases just after the second return stroke, which occurs at approximately 0.5 seconds or midway through the time interval colored green. This point in time coincides with the time when profuse branching of the positive leader begins (compare Figure 12 with the right panel of Figure 9). This coincidence indicates that there may be a correlation between growth rate and CC. However later in the flash, just before the return stroke with long CC begins, there is a drop in growth rate, which coincides with a decrease in branching. The fact that the growth rate decreases during the longest CC supports our earlier observation that CC duration does not depend in any simple way on the growth rate of the positive leader.

In summary, seven of nine flashes showed no significant variation in positive-channel growth rate, despite the instance of CC. Even though two of nine flashes do have non constant growth rates, these showed trends that were inconsistent with the speculation that the growth of the positive leader is the source of CC. While some increases in growth rates did coincide with the occurrence of CC, others did not. Also, there were instances where long CC was accompanied by lower growth rates than shorter duration CC.

4. Conclusions

Using LEFA data to find CC duration and the PulseGraph function to estimate channel growth vs time, the growth of positive leaders was compared to CC occurrence and duration. Plotting growth vs CC duration for individual return strokes indicates that the positive leader grows at a constant rate. Using the growth rate, obtained from the linear slope of this plot, we were able to estimate the velocity of the positive leader, which agrees with previous values reported in the literature.

The average growth rate during each return stroke, including CC duration, was calculated. Each return stroke was then categorized by their average growth rate and compared by their CC type (long, short, very short, or no CC). We found no significant difference in growth rate based on CC type.

The growth rate throughout a flash during 10 ms windows was analyzed for the nine flashes in this study. Seven out of the nine flashes contained constant growth rates during positive leader activity even though there were occurrences of CC, while the remaining two flashes showed peaks which are inconsistent with CC occurrence.

It is possible that CC is caused by growth that occurs on a small scale unresolved by the LMA. However, the observations in this study all agree with the following: the growth of the positive leader is not the primary mechanism determining CC occurrence and duration. Therefore, there must be some other mechanism that determines the occurrence and duration of CC.

Most of the recent papers concerning continuing current focus on observations and assume that the mechanism is known. As mentioned in Section 1.2, many researchers believe that the source of CC comes from the growth of the positive leader, therefore studies into other mechanisms as the source of CC are lacking. *Heckman* [1992] does a thorough analysis of why some lightning flashes get cut-off and produce multiple return strokes and some produce CC, or both. However, he also assumes that the current source is provided by the positive leader growth. Similarly, *Mazur* [2002] models how the bottom layers of branching can screen upper branches from the ground electric field and result in the cutoff of the channel to ground, but again assumes that the source of current comes from the channel growth. Our current findings indicate that more thought must be dedicated to alternate mechanisms of continuing current.

Acknowledgments. Raw data and scripts to reproduce the figures presented in this paper may be found at www.physics.nmt.edu/∼rsonnenf/papers/2014CCandLEADERS/ This work was funded by grant CMB-0724750 from the National Science Foundation. Additional funding was obtained from the DARPA-NIMBUS program. We gratefully acknowledge Vaisala Corporation for providing access to precision National Lightning Detection Network data. We thank the National Forest Service for the use of land at Langmuir Laboratory and the Bureau of Land Management for allowing siting of LEFA stations on Federal land.

References

Ballarotti, M. G., M. M. F. Saba, and O. P. Jr, High-speed camera observations of negative ground flashes on a millisecond-scale, *Geophys. Res. Lett.*, *32*, L23,802, doi: 10.1029/2005GL023889, 2005.

Brook, M., N. Kitagawa, and E. J. Workman, Quantitative study of strokes and continuing currents in lightning discharges to ground, *J. Geophys. Res.*, *67*, 649–657, 1962.

Edens, H. E., et al., VHF lightning mapping observations of a triggered lightning flash, *Geophys. Res. Lett.*, *37*, L19,807, doi:10.1029/2012GL053666, 2012.

Hager, W. W., R. G. Sonnenfeld, B. C. Aslan, G. Lu, W. P. Winn, and W. L. Boeck, Analysis of charge transport during lightning using balloon-borne electric field sensors and lightning mapping array, *J. Geophys. Res.*, *112*, D18,204, doi:10.1029/2006JD008187, 2007.

Heckman, S. J., Why does a lightning flash have multiple strokes?, Ph.D. thesis, Massachusetts Institute of Technology, 1992.

Kitagawa, N., M. Brook, and E. J. Workman, Continuing currents in cloud-to-ground lightning discharges, *J. Geophys. Res.*, *67*, 637–647, 1962.

Krehbiel, P. R., M. Brook, and R. A. McCrory, An analysis of the charge structure of lightning discharges to ground, *J. Geophys. Res.*, *84*(C5), 2432–2456, 1979.

Lu, G., W. Winn, and R. G. Sonnenfeld, Charge transfer during intracloud lightning from a time-dependant multidipole model, *J. Geophys. Res.*, *117*, 16, doi: 10.1029/2010JD014495, 2011.

Mazur, V., Physical processes during development of lightning flashes, *C. R. Physque*, *3*, 1393–1409, 2002.

Rakov, V. A., and M. A. Uman, Long continuing current in negative lightning ground flashes, *J. Geophys. Res.*, *95*(D5), 5455–5470, 1990.

Rakov, V. A., and M. A. Uman, *Lightning Physics and Effects*, Cambridge University Press, Cambridge, 2003.

Rison, W., R. Thomas, P. Krehbiel, T. Hamlin, and J. Harlin, A gps-based three-dimensional lightning mapping system: Initial observations in central new mexico, *Geophys. Res. Lett.*, *26*(23), 3573–3576, 1999.

Ross, M., S. A. Cummer, T. K. Nielsen, and Y. Zhang, Simultaneous remote electric and magnetic field measurements of lightning continuing currents, *J. Geophys. Res.*, *113*, D03,101, doi:10.1029/2008JD010294, 2008.

Saba, M. M. F., M. G. Ballarotti, and O. P. Jr., Negative cloud-to-ground lightning properties from high speed video observations, *J. Geophys. Res.*, *111*, D03,101, doi:

10.1029/2005JD006415, 2006a.

Saba, M. M. F., O. P. Jr., and M. G. Ballarotti, Relationship between lightning return stroke peak current and following continuing current, *Geophys. Res. Lett.*, *33*, L23,807, doi:10.1029/2006GL027455, 2006b.

Shindo, T., and M. A. Uman, Continuing current in negative cloud-to-ground lightning, *J. Geophys. Res.*, *94 D4*, 5189–5198, 1989.

Sonnenfeld, R. G., and W. W. Hager, Electric field reversal in sprite electric field signature, *Mon. Weather Rev.*, *141*, 1731–1735, doi:10.1175/MWR-D-12-00220.1, 2013.

Thomas, R. J., P. R. Krehbiel, W. Rison, S. J. Hunyady, W. P. Winn, T. Hamlin, and J. Harlin, Accuracy of the Lightning Mapping Array, *J. Geophys. Res.*, *109*, D14,207, doi:10.1029/2004JD004549, 2004.

van der Velde, O. A., and J. Montanyà, Aircraft observations of a lightning channel in steps, *J. Geophys. Res.*, *118, 13*, 504–13, 519, doi:10.1002/2013JD020257, 2013.

Warner, T., J. H. H. Jr., and A. G. Detwiler, Aircraft observations of a lightning channel in steps, *Geophys. Res. Lett.*, *30*, 19, doi:10.1029/2003GL017334, 2003.

Williams, E. R., Problems in lightning physics - the role of polarity asymmetry, *Plasma Sources Science and Technology*, *15*, S91–S108, doi:10.1088/0963-0252/15/2/S12, 2006.

Yoshida, S., et al., Three-dimensional imaging of upward positive leaders in triggered lightning using vhf broadband digital interferometers, *Geophys. Res. Lett.*, *37*, L05,805, doi:10.1029/2009GL042065, 2010.

Table 1. Summary of CC definitions

Definition	**Duration (ms)**
Very Short	3-10
Short	10-40
Long	> 40

Table 2. Comparison of CC durations for 14 August 2012 flash as detected from multiple LEFA stations

Inst. #	**RS1 (ms)**	**RS2 (ms)**	**RS3 (ms)**	**RS4 (ms)**	**RS5 (ms)**	**RS6 (ms)**	**RS Distance (km)**
LEFA5	5.8	4.4	29.3	35.3	157	3.5	25.0
LEFA3	5.5	2.5	42.9	28.9	142	2.7	29.4
LEFA7*	10.0	4.3	31.0	22.2	156	3.5	30.9
LEFA8	5.0	5.0	33.9	23.6	158	2.6	32.8
LEFA10	6.7	4.1	32.7	19.2	159	3.5	33.8
LEFA6*	3.9	2.7	23.1	15.8	101	1.5	35.6

*These instruments were noisy due to their proximity to power lines, and therefore provide much less reliable durations.

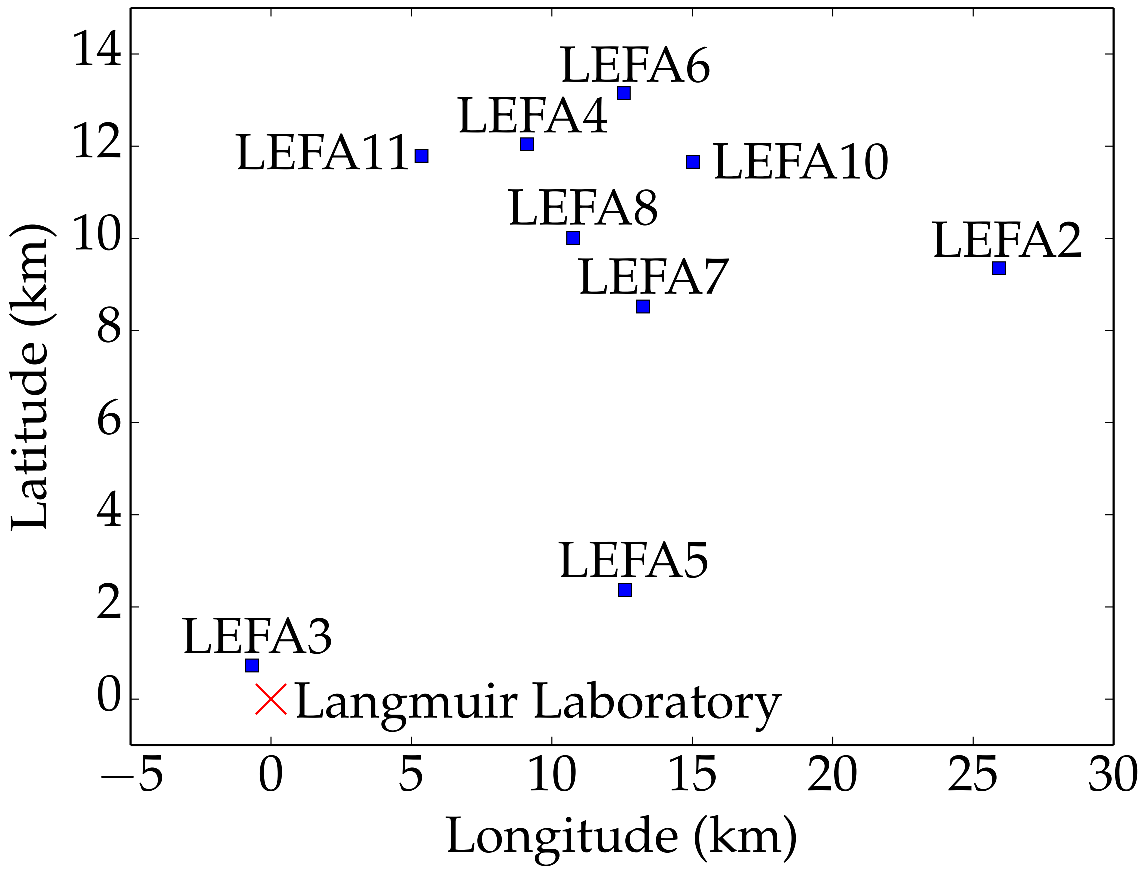

Figure 1. Figure illustrating the locations of the LEFA stations. Langmuir Laboratory is used as the origin for all the figures in this paper, which is labeled with a red X. LEFA2 is located on the campus of New Mexico Institute of Mining and Technology.

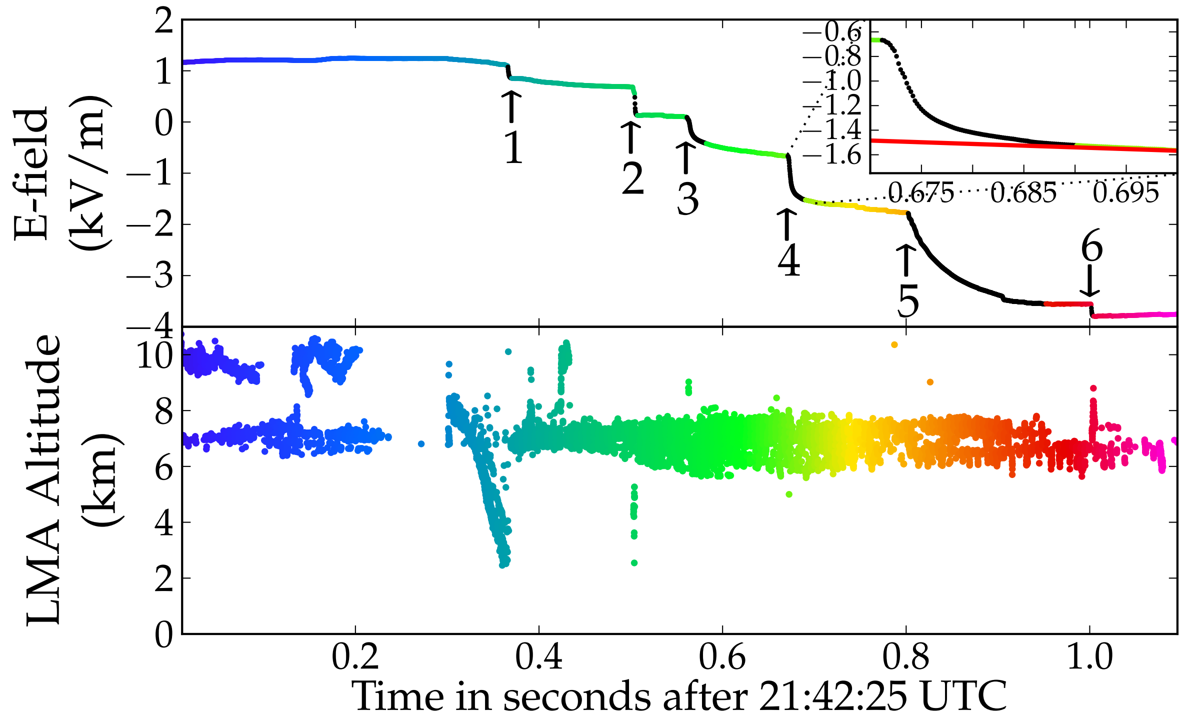

Figure 2. LEFA (top panel) and LMA (bottom panel) data for a bolt-from-the-blue flash occurring on 14 August 2012. This figure illustrates the method used to determine CC duration. The flash had six return strokes, three of which had CC (3, 4, and 5). The LMA data shows that most of the breakdown activity occurring after the first return stroke is in the negative charge region, which is caused predominately by positive leader breakdown. Color represents time from initiation of flash. The black line segments represent the duration of CC. The top inset demonstrates the technique used to identify the end of CC, which is determined by the point where the electric field and linear fit intersect.

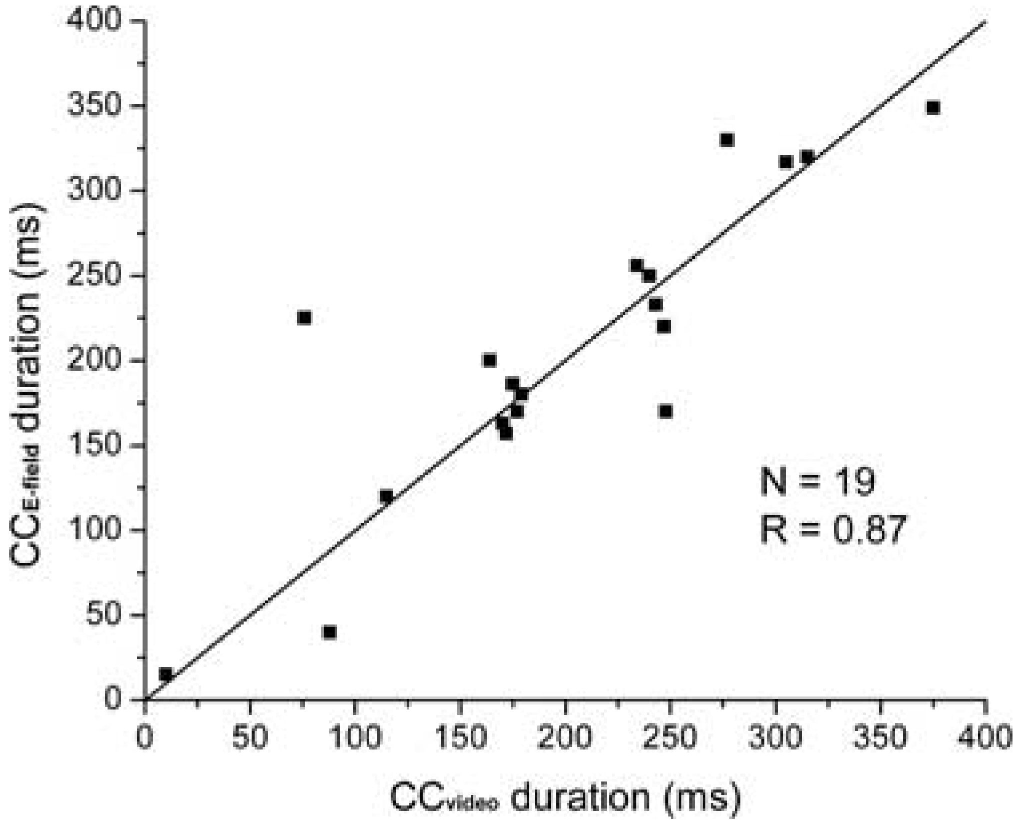

Figure 3. Comparison between CC duration measured using electric field data and high-speed video data for 19 return strokes (figure from *Saba et al.* [2006b], used with permission). This result indicates that E-field measurements are an adequate proxy for estimating CC durations.

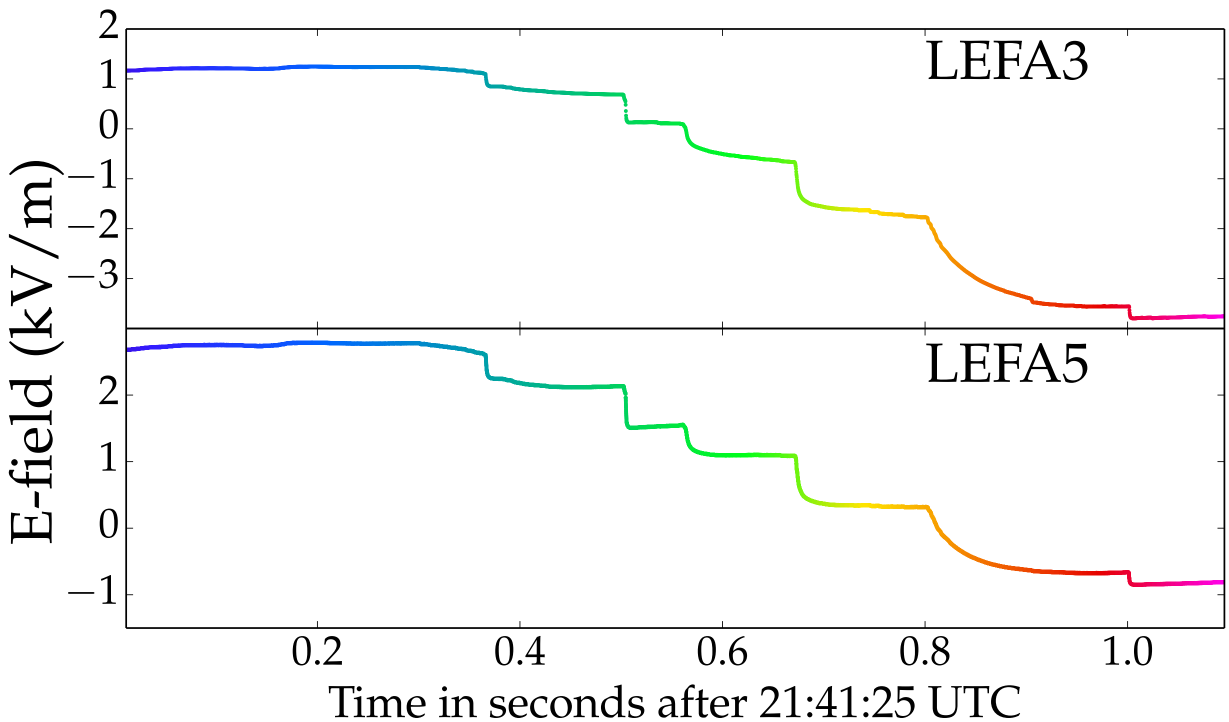

Figure 4. Electric field data from LEFA3 (top) and LEFA5 (bottom). The direction of the positive leader for this flash is moving at different directions compared to the location of each station (compare Figures 1 and 5). Since the sign of the electric field change is the same for each station, one can be confident that the electric field change is caused be CC and not the motion of the positive leader.

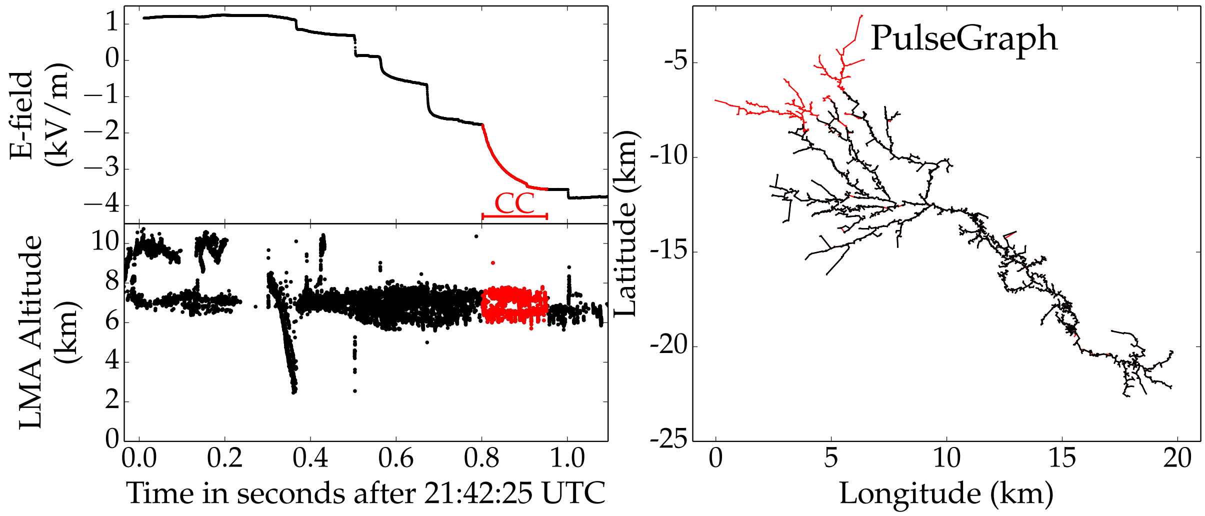

Figure 5. LEFA (top left), LMA VHF source altitude (bottom left), PulseGraph output (right) for bolt-from-the-blue flash occurring on 14 August 2012. This figure illustrates the method used to determine positive-channel growth during CC. Red on the PulseGraph plot indicates new channel growth during the time of the fifth return stroke (indicated also in red on the LEFA and LMA plots).

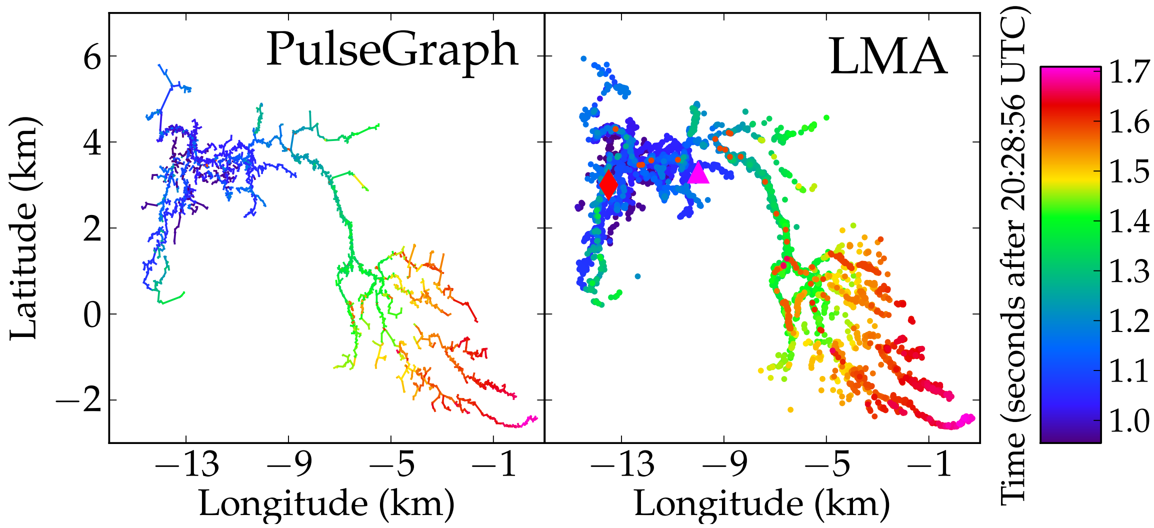

Figure 6. LMA (right) and PulseGraph (left) plan views of –CG flash occurring at 20:28:56 UTC on 8 July 2013. This figure demonstrates that the PulseGraph algorithm correctly fits the branch structure found in the LMA data. Color represents time (shown in colorbar). The magenta triangle designates the location of the first return stroke while the red diamond represents the location of the rest of the return strokes according to NLDN data.

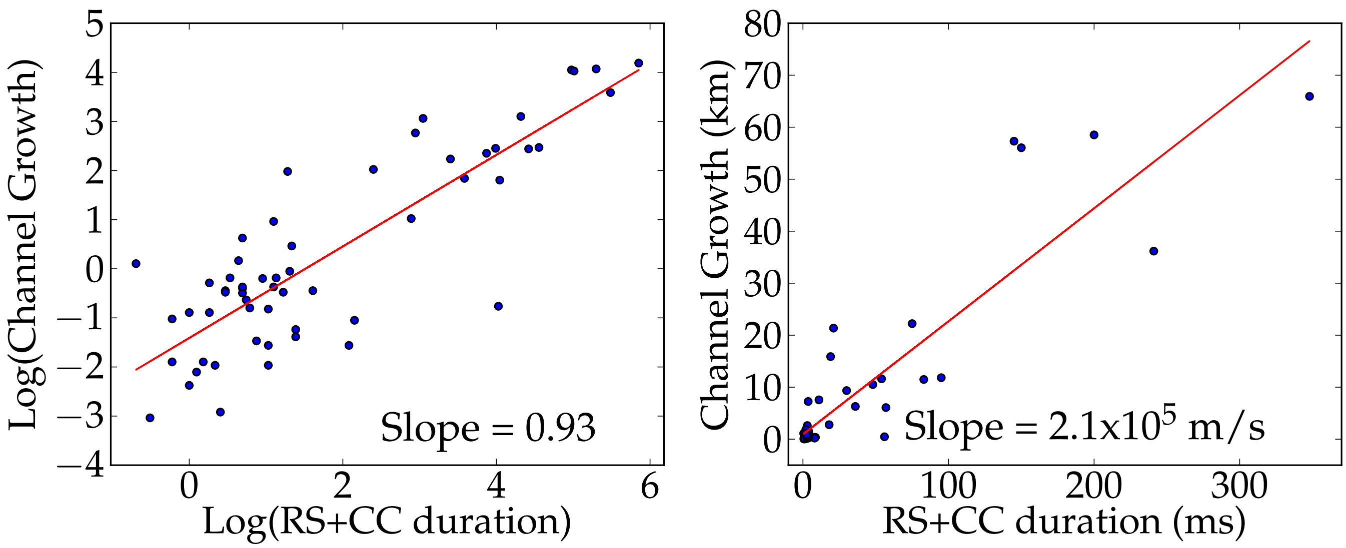

Figure 7. Plot of channel growth vs CC duration depicted as a base 10 log-log plot (left) and linear plot (right) for 9 flashes with a total of 57 return strokes. The log-log plot illustrates that the data follows a power law function, with the power being 0.93, or nearly linear. The slope in the linear plot represents the cumulative speed of all the branches in the positive leader. This cumulative speed is used to estimate the velocity of each individual positive leader branch.

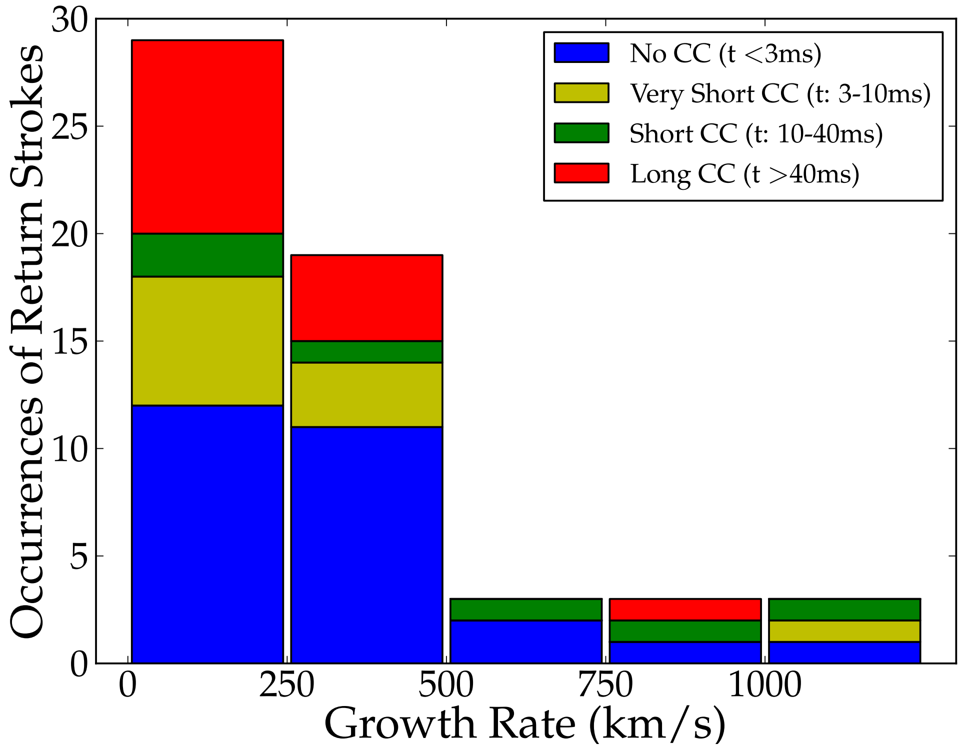

Figure 8. Histogram of return strokes categorized by growth rate. The y-axis shows the number of return strokes (from our data set of nine flashes) that had positive-channel growth rates indicated on the x-axis. The red, green, and yellow bars count long, short, and very short CC (as described in Table 1), while the blue bars represent no measurable CC (lasting less than 3 ms). The data reveals no preferential growth rate based on CC type.

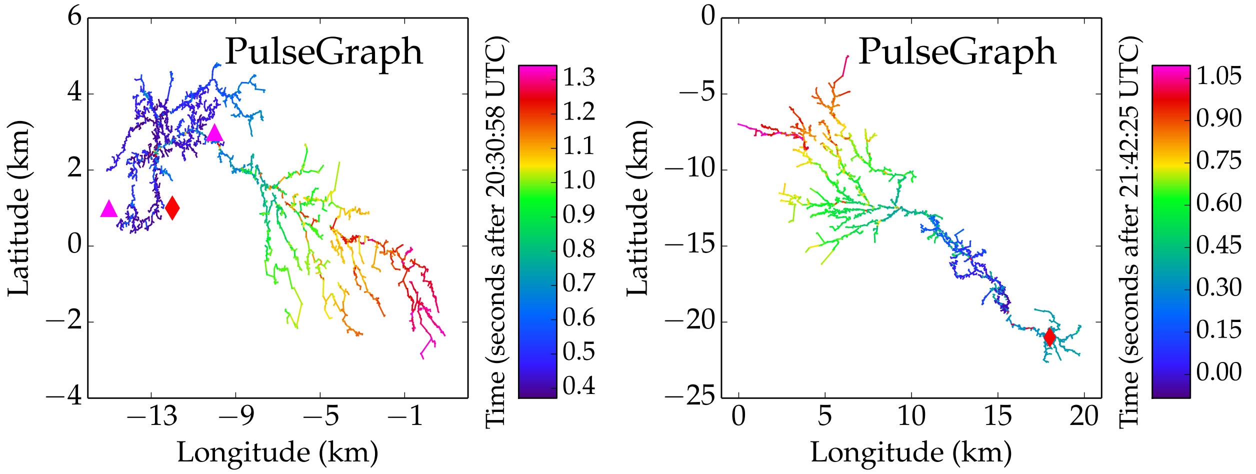

Figure 9. PulseGraph plan views of –CG flash occurring at 20:30:58 UTC on 8 July 2013 (left) and a bolt-from-the-blue flash occurring at 21:42:25 UTC on 14 August 2012 (right). Color represents time (shown in colorbars). The magenta triangles represent single return stroke locations, while red diamond designates the location of all the subsequent return strokes of that flash according to NLDN data. These PulseGraphs were used to calculate the growth rates for Figures 11 and 12.

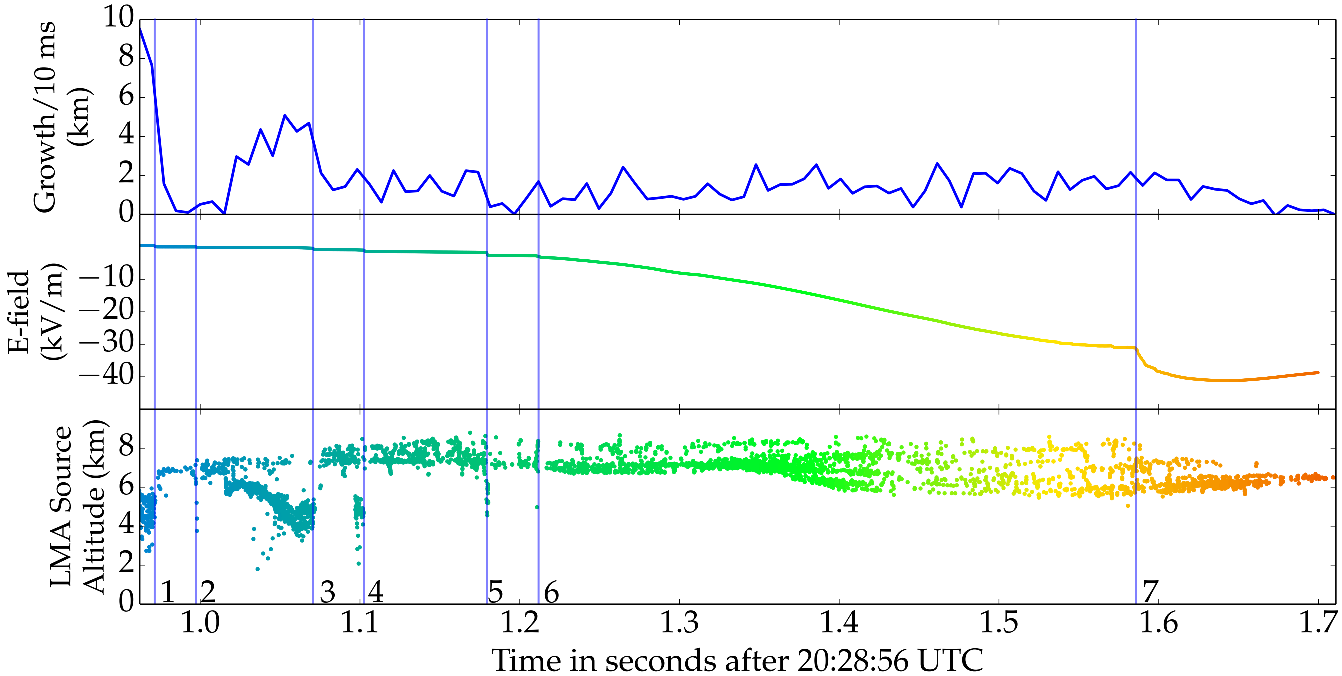

Figure 10. Growth calculated over 10 ms windows throughout the flash (top). LEFA (middle) and LMA (bottom) data matched in time for a –CG flash occurring on 8 July 2013. This flash has seven return strokes (highlighted by vertical blue lines and sequentially numbered) according to NLDN data. Once the final negative stepped leader connects to ground, the positive-channel growth rate remains constant even though CC occurs.

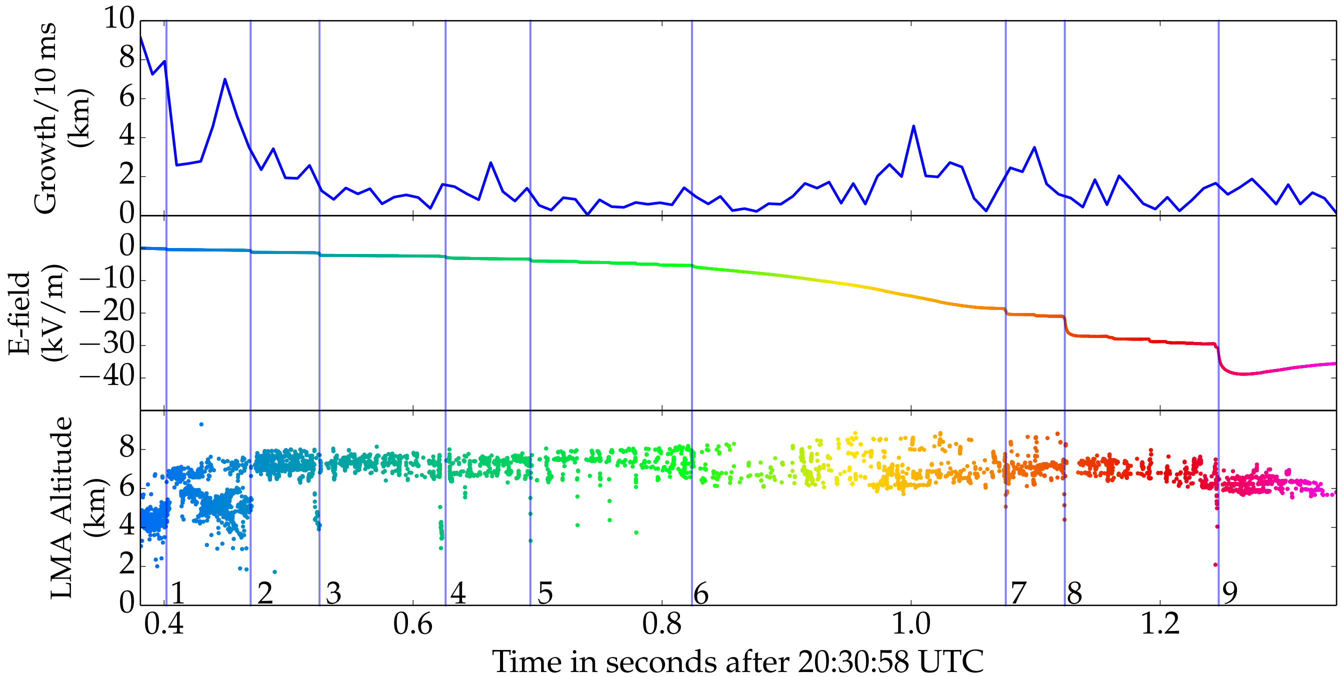

Figure 11. Growth calculated over 10 ms windows throughout the flash (top). LEFA (middle) and LMA (bottom) data matched in time for a –CG flash occurring on 8 July 2013. This flash has nine return strokes (highlighted by vertical blue lines and sequentially numbered) according to NLDN data. Once the final negative stepped leader connects to ground, the positive-channel growth remains relatively constant until approximately 0.9 s. This is true even though the sixth return stroke is followed by long CC. Also, although the seventh return stroke does not initiate CC, there is a peak in growth rate between the seventh and eighth return stroke.

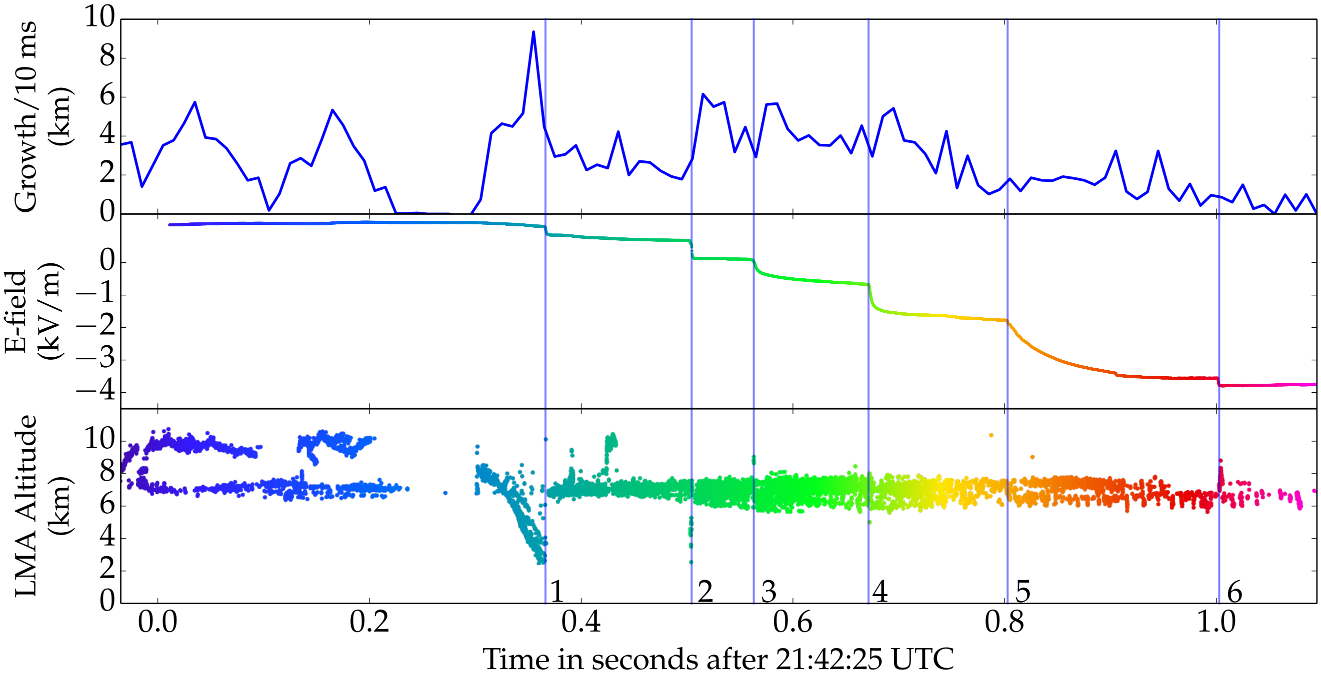

Figure 12. Growth calculated over 10 ms windows throughout the flash (top). LEFA (middle) and LMA (bottom) data matched in time for a bolt-from-the-blue flash occurring on 14 August 2012. This flash has six return strokes (highlighted by vertical blue lines and sequentially numbered) according to NLDN data. By comparing this data with Figure 9 it is apparent that the growth rate increases when the number of active branches increases.